FIRST EXPERIMENTS OF SECTOR INTERPOLATED SAR TOMOGRAPHY

Fabrizio Lombardini, Matteo Pardini

Dept. of Information Engineering – University of Pisa
Via G. Caruso, 16 – 56122 – Pisa – Italy
{f.lombardini, matteo.pardini}@iet.unipi.it

1. INTRODUCTION

Synthetic aperture radar 3-D Tomography (Tomo-SAR) is an experimental multibaseline (MB) extension of conventional cross-track SAR interferometry employing many (on the order of ten) passes over the same area. Through the coherent combination of MB data at the complex (i.e. amplitude and phase) data level, Tomo-SAR can separate multiple scatterers at different heights in each given range-azimuth cell, and produces a continuous reflectivity profiling along the height direction (h–direction). Generally speaking, Tomo-SAR exploits an aperture in the height-range plane constituted by the MB geometry to get full 3-D imaging through elevation beam forming (spatial spectral estimation). Applications of Tomo-SAR have been found for biomass estimation, forest classification, tree and building height estimation, and other geophysical parameter extraction problems [1].

However, in practice possible temporal decorrelation of the scattering and problems of cost prevent from using a large number of passes, while navigation/orbital considerations do not allow obtaining ideal planned uniformly spaced parallel flight tracks. As a consequence, the point spread function (PSF) along the h–direction is distorted. In particular, the non-uniform baseline (spatial) sampling causes bad h-imaging quality results with the classical Fourier-based focusing in terms of contrast and ambiguities, as anomalous side and quasi-grating lobes affect the PSF. Alternatively to the Fourier-based processing, a regularized inversion approach to Tomo-SAR was first introduced in [2], whereas in [3] an adaptive beamforming technique was proposed and tested, providing strong height super-resolution and sidelobe suppression capabilities. As a drawback, the adaptive processing is sensitive to residual data miscalibration, and it exhibits radiometric non-linearities. Also, to operate it needs a spatial coherent multilooking, i.e. it does not operate at full horizontal resolution. More recently, other solutions have been also proposed and tested for the 3-D focusing and parameter extraction [4]-[8].

In a different class of tomographic processors, the MB data are pre-processed by filling the gaps in the available baseline distribution. Under the simplifying assumption that a single height backscattering contribution is dominant in the range-azimuth cell, a simple gap filling algorithm has been proposed in [1]. However, unsatisfactory results are obtained in scenarios comprising more than one point-like spaced or extended scatterer [9], because of the assumption mismatch. An extension of the interpolator in [1] to more general scenarios has

been proposed in [10]. This advanced "knowledge-based" interpolator exploits an a priori information about the extension of a height sector containing all the scatterers (the so-called sector of interest, SOI). The achievable good imaging quality has been shown with simulated data [10].

In this work, first experiments of 3-D focusing are presented with the advanced sector interpolator applied to real MB SAR data. We show that with well interpolated data the performance limitations intrinsic in a MB sparse geometry tend to vanish, and the height tomographic image can be obtained simply by applying the classical Fourier elevation focusing to the interpolated data. The overall processing chain is thus capable to reduce the sidelobe amplitudes and at the same time it is radiometrically linear, which is desirable in some geophysical applications. In addition to that, sidelobe cleaning still holds even with full horizontal resolution processing (for which the adaptive focusing is not operative), making the sector interpolator a valid pre-processing step for the 3-D analysis of urban scenarios.

2. BASICS OF SECTOR INTERPOLATION AND FIRST RESULTS

The sector interpolation algorithm is applied after the conventional deramping and possible atmospheric compensation [2]. Basically, the algorithm derives an interpolation matrix $\mathbf{H}_I$ according to the following design criterion [10]:

$$\mathbf{H}_I = \arg\min_{\mathbf{H}} \int_{SOI} \left\| \mathbf{a}_V(h) - \mathbf{H}\mathbf{a}(h) \right\|^2 dh \,,$$

where $\mathbf{a}_V(h)$ and $\mathbf{a}(h)$ are the virtual (ideal uniform) and actual (non uniform) MB array responses viz. steering vectors [10], respectively, calculated for the same heights inside the sector of interpolation. The solution to this optimization problem is available in closed form. Then, the interpolated MB data vector is calculated as $\mathbf{y}_I = \mathbf{H}_I \mathbf{y}$, where vector $\mathbf{y}$ contains the available non-uniform MB data. So doing, the non-uniform spatial samples of all the spatial harmonics corresponding to the height reflectivity distribution are well interpolated, provided that their frequencies fall into the sector assumed in the interpolation matrix design. After the linear interpolation, the tomographic profile is derived by means of the classical uniform Fourier beamforming.

The sector interpolator has been applied to ERS-1/2 data over the suburban area of "Cinecittà" of the city of Rome. In these experiments, an improved (robustified) version of the sector interpolator has been used to handle miscalibration residuals. The dataset consists of 40 images acquired between 1995 and 2000. The baseline distribution is highly non-uniform, with an overall orthogonal baseline of about 1500m. From rough a priori information of the urban scenario at hand and possibly previous analyses of the area [11], we assume that the scattering is comprised in a SOI extending from -20m to 40m with respect to the deramping height reference. In Fig. 1, sample results of the obtained tomographic profiles are shown before and after the sector interpolation. The former case is labelled with "NLA data", where the NLA acronym stands for non-uniform linear array. Results for two different single look cells are reported. In Fig. 1(a) the profiles are plotted for a single scatterer

located at a height of 3m, whereas Fig. 1(b) refers to a cell with two scatterers, located approximately at 16m and 25m. In both cases, the improved quality of the profile from the sector interpolated data is apparent, with gains in the peak sidelobe level of about 3dB for the single scatterer and 4dB for the double scatterer.

In the full paper, further results of sector interpolated tomography applied to urban spaceborne data will be shown, possibly with comparisons with other linear focusing techniques. Moreover, other experiments testing radiometric linearity of sector interpolated tomography will be also reported, by applying the method to airborne data of forest scenarios. Finally, sector knowledge-based algorithmic solutions will be proposed to obtain a height resolution better than the Rayleigh limit imposed by the Fourier focusing even with single look processing.

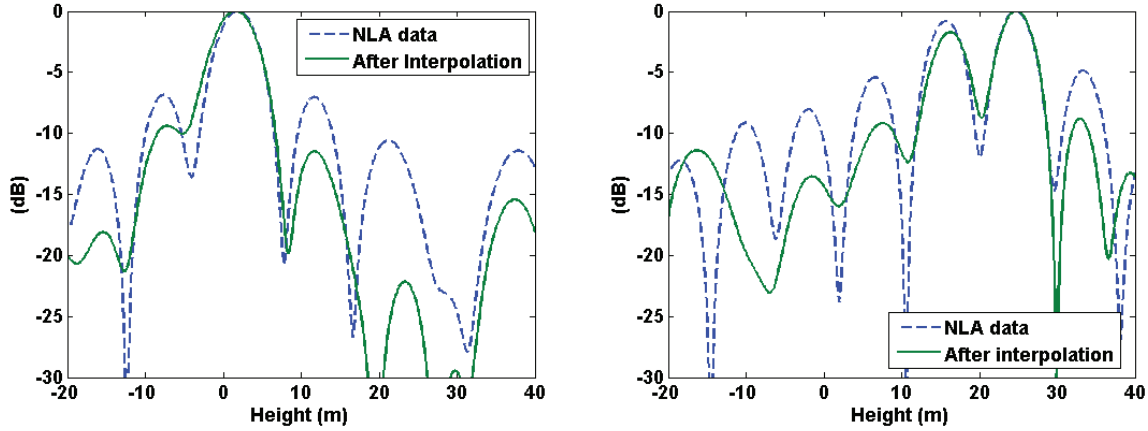

(a) (b)

Figure 1 – Normalized tomographic profiles obtained with the classical Fourier focusing before (dashed blue curve) and after (solid green curve) the sector interpolation, ERS-1/2 urban data. (a) Single scatterer; (b) Double scatterer. Single look processing. The authors wish to thank Dr. Fornaro from CNR-IREA for providing the calibrated dataset.

3. REFERENCES

[1] A. Reigber, A. Moreira, "First Demonstration of Airborne SAR Tomography Using Multibaseline L-Band Data," *IEEE Trans. Geosci. Remote Sens.*, vol. 38, no. 5, pp. 2142-2152, May 2000.

[2] G. Fornaro, F. Serafino, F. Soldovieri, "Three Dimensional Focusing with Multipass SAR," *IEEE Trans. Geosci. Remote Sens.*, vol. 41, no. 3, pp. 507-517, Mar. 2003.

[3] F. Lombardini, A. Reigber, "Adaptive Spectral Estimation for Multibaseline SAR Tomography with Airborne L-Band Data," *Proc. IEEE IGARSS 2003*, pp. 2014-2016, Jul. 2003.

[4] F. Lombardini, J. Ender, L. Roessing, M. Galletto, L. Verrazzani, "Experiments of Interferometric Layover Solution With the Three-Antenna Airborne AER-II SAR System," *Proc. IEEE IGARSS 2004*, pp. 3341-3344, Sep. 2004.

[5] S. R. Cloude, "Dual-Baseline Coherence Tomography", *IEEE Geosci. Remote Sens. Letters*, vol. 4, no. 1, pp. 127-131, Jan. 2007.

[6] X. Zhu, N. Adam, R. Bamler, "First Demonstration of Spaceborne High Resolution SAR Tomography in Urban Environment Using TerraSAR-X Data," *Proc. CEOS Workshop*, Nov. 2008.

[7] S. Tebaldini, F. Rocca, A. Monti Guarnieri, "Model Based SAR Tomography of Forested Areas," *Proc. IEEE IGARSS 2008*, pp. 593-596, Jul. 2008.

[8] A. Budillon, A. Evangelista, G. Schirinzi, "SAR Tomography From Sparse Samples," *Proc. IEEE IGARSS 2009*, Jul. 2009.

[9] G. Fornaro, F. Lombardini, F. Serafino, "Three-Dimensional Multipass SAR Focusing: Experiments With Long Term Spaceborne Data," *IEEE Trans. Geosci. Remote Sens.*, vol. 43, no. 4, pp. 702-714, Apr. 2005.

[10] F. Lombardini, M. Pardini, "3-D SAR Tomography: The Multibaseline Sector Interpolation Approach," *IEEE Geosci. Remote Sens. Letters*, vol. 5, no. 4, pp. 630-634, Oct. 2008.

[11] F. Lombardini, M. Pardini, G. Fornaro, F. Serafino, L. Verrazzani, M. Costantini, "Linear and Adaptive Spaceborne Three-dimensional SAR Tomography: A Comparison on Real Data", *IET Radar, Sonar and Navigation*, vol. 3, no. 4, pp. 424-436, Aug. 2009.